

# A Study on Reducing Gear Tooth Profile Error by Finish Roll Forming

Seizo Uematsu, Donald R. Houser, Sung-Ki Lyu,  
Long Lu, Ju-Suck Lim

## Introduction

This paper deals with the tooth profile error of spur gears that have been finished by roll forming. First, we present experimental data that confirms that the tooth profile error is a synthesis of a concave error and a pressure angle error (Refs. 7–8). Since various types of tooth profile errors appear in the experiments, evaluation parameters are introduced for rolling gears so that profile quality may be objectively evaluated. Using these evaluation parameters, the relationships among the tooth profile error, the addendum modification factor (A.M. factor) and the tool loading force are verified.

The character of concave error, pressure angle error and tool loading force of finish roll forming by using a forced displacement method are verified. This study makes clear that the tool loading force of finish roll forming is a very important factor that affects involute tooth profile error.

## Evaluation Parameters for Roll Forming

Figure 1 shows the evaluation parameters for gear rolling. The parameters are maximum deformation  $\delta_{max}$ , concave deformation  $\delta_{ca}$ , deformation at tooth tip  $\delta_T$  and pressure angle error  $\delta_\alpha$ . The solid and broken lines in the figure indicate the tooth profile curves before and after rolling, respectively.  $\delta_{max}$  is the

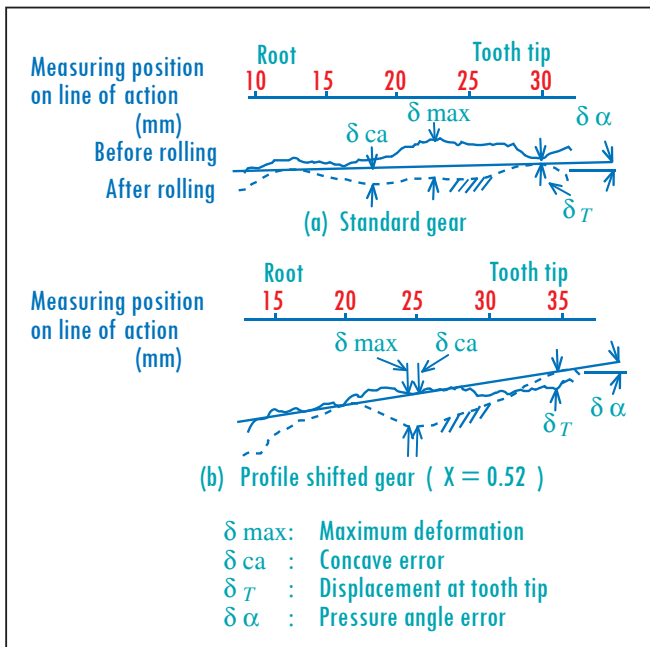


Figure 1—Plastic deformation on tooth profile.

## Management Summary

In recent years, the gear industry is increasingly applying non-cutting forming methods to the production of toothed workpieces. Of these, finish roll forming seems to have the widest range of application. Finish roll forming is a manufacturing technology that improves the tooth profile accuracy, pitch accuracy and surface roughness of a hobbed gear. In this technique, a hobbed gear having a finish roll stock allowance contacts under high load with a tool having a high accuracy profile. The high load plastically deforms the surfaces of the teeth, smoothing them and making them more accurate. This concept was proposed by Ford Motor Co. for the finishing of automotive pinions (Ref. 1).

Based on the proposed concept, automotive gear manufacturers attempted finish rolling larger gears, but could not obtain adequate quality. A great deal of research and development work has been carried out by many companies and researchers to see if roll forming can be more widely applied to larger gears with coarser pitches (Refs. 2–6). However, these investigators could not develop a mechanism to generate high quality profiles.

In this study, the authors have developed a rack-type rolling process in which a rack tool is used to roll gear teeth. The results of the experiment and analysis show that the proposed method reduces errors.

**Dr. Seizo Uematsu** is a retired member of the engineering faculty at Yamagata University, located in Shimowada, Japan. In 2002, he retired from the university's precision engineering department. He's studied roll forming of gears for more than 30 years, publishing 14 papers on the subject.

**Dr. Donald R. Houser** is director of the Gear Dynamics and Gear Noise Research Laboratory (GearLab), located at The Ohio State University in Columbus. GearLab is an industrially sponsored research consortium with 30 participating companies. Houser is also a professor in the university's mechanical engineering department. He teaches and researches in the areas of gear design and gear manufacture.

**Dr. Sung-Ki Lyu** is director of the Regional Consortium Center, located at Gyeongsang National University in Jinju, South Korea. The center performs industrial research sponsored by 20 participating companies. Lyu is also a professor in the university's mechanical & aerospace engineering department. He teaches and researches in the area of gear design.

**Dr. Long Lu** is a professor in the mechanical engineering department of the Huaihai Institute of Technology, located in Lianyungang, China. He earned his doctorate at Gyeongsang National under Dr. Lyu's supervision.

**Ju-Suck Lim** is a graduate student at Gyeongsang National studying finish roll forming of gears.

value of deformation at the position of maximum deformation when the tooth profile curves are compared before and after rolling a gear.  $\delta_{ca}$  is the value of deformation at the position of the maximum distance from the tangent line to the profile where a tangent is drawn through the tooth tip and tooth root on the profile.

A positive value of  $\delta_{ca}$  indicates a concave shape on the tooth profile, whereas a negative value indicates a convex shape.  $\delta_T$  is the amount of deformation at tooth tip. A positive value of  $\delta_T$  is the form in which the tooth tip is lower before rolling and a negative value is the opposite form.  $\delta_\alpha$  is the pressure angle error.

#### Test Gear and Experimental Method

The experiment was conducted on module 5 spur gears as follows: A rack was used for the tool and was driven at a speed of 4.5 mm/min. (0.08 mm/sec.). The number of teeth on the gear was 22 and the A.M. factor was 0.52.

The specifications of the roll forming tool and the test gears are shown in Table 1. The shape of the test gears is shown in Figure 2 and in Photo 1. The gear on the left side of the photo is a standard gear, and the gear on the right is one of the roll formed gears made in this study. The rolling was performed

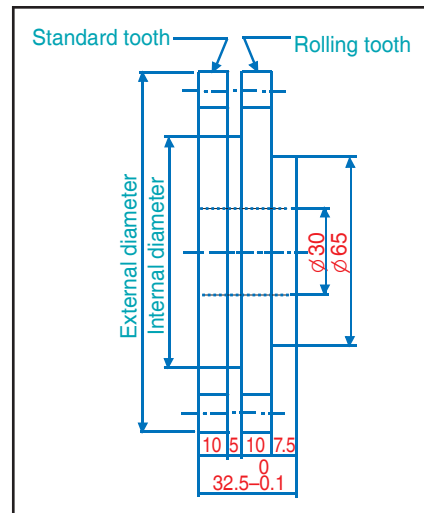


Figure 2—Shape of test gear.



Photo 1—Test gear.

Table 1—Specification of Roll Forming Tool and Test Gears.

	Tool	Test gear
Module (m)	5	
Number of teeth (z)	11	22
Pressure angle (deg)	20°	
Tooth width (mm)	17.5	10
Coefficient of profile shift		0.52
External diameter (mm)		125
Material	SK5	S45C
Hardness	HRC 63	HRB 80
Individual pitch (μm)	1.0	7
Cumulative pitch (μm)	1.0	20

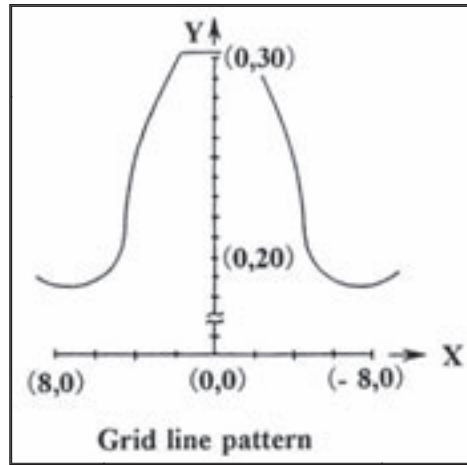


Figure 3—Method of tooth deflection measurement.

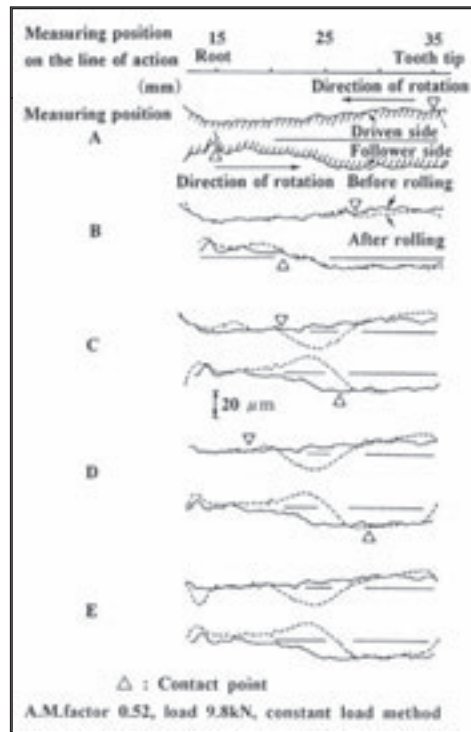


Figure 4—Variation of tooth profile in rolling process.

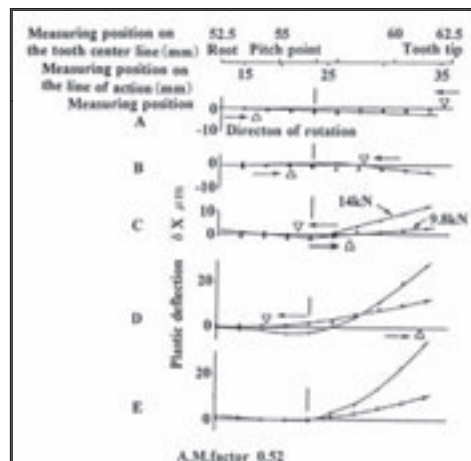


Figure 5—Plastic deflection of tooth.

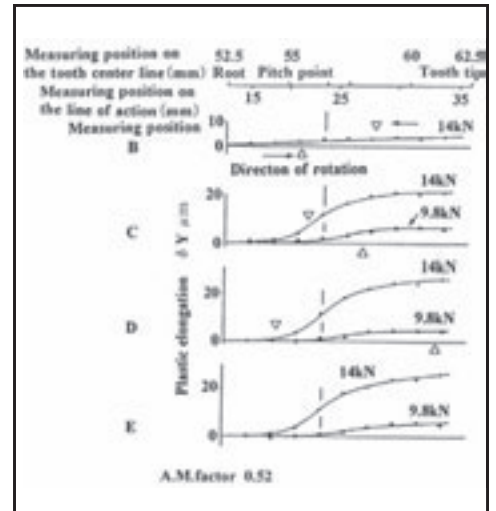


Figure 6—Plastic elongation on the tooth center line.

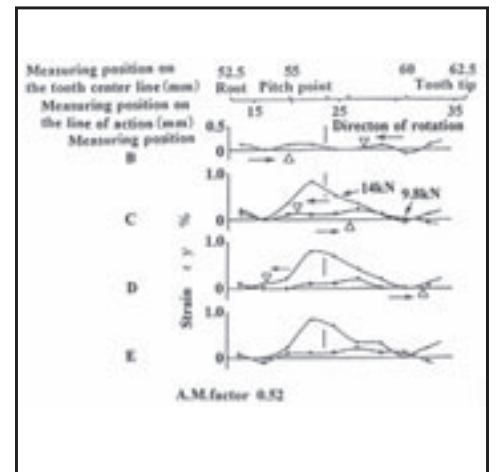


Figure 7—Strain distribution on the tooth center line.

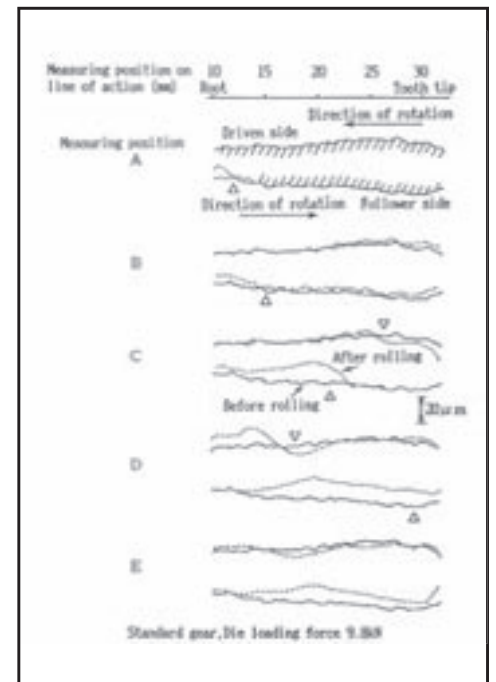


Figure 8—Variation of tooth profile in rolling process.

over several teeth and was repeated several times on the same teeth. The tooth profile and tooth trace curves were measured after each rolling cycle. After rolling, the evaluation parameters were compared to those of the standard tooth.

### Deformation Mechanism

If the amount of deformation becomes partially negative on a tooth profile, this phenomenon cannot be explained by analytical methods based on the amount of deformation. Therefore, the teeth seem to bend plastically during rolling. The formation mechanism of the pressure angle error was studied as follows: Since a large portion of the roll stock plastic deformation occurs during the first rolling pass, the remainder of the discussion will focus on results after the first rolling pass.

For verification, the profile of mating tooth and the displacements of lattice point drawn on the side of the tooth were measured at several positions on the line of action. Therefore, we stopped the mating gear at several positions on the line of action. During rolling, each measuring position on the line of action was judged by comparing the output from the strain gage at the tool's tooth root and the analytical mating diagram. Since the tool driving speed is 0.08 mm/sec., the tool can be stopped near a target position.

Figure 3 shows the lattice points drawn on the tooth side. The lattice points are arranged on the mirror-finished side of the tooth using the micro Vickers tester. In the coordinate system on the tooth side, the Y-axis is positioned on the centerline of the tooth side and the origin is positioned 30.5 mm from the tooth tip on the centerline. The X-axis is the direction perpendicular to the centerline. The lattice point interval  $\Delta$  is set to 1 mm. The components of the displacement of the lattice point are  $\delta_x$ ,  $\delta_y$  in each axis. The plastic strain  $\epsilon_y$  between lattice points on the centerline direction was defined as follows:

$$\epsilon_{yi} = (\delta_{yi} - \delta_{yi-1})/\Delta \quad (1)$$

where index  $i$  indicates the position of a lattice point from the origin on the centerline.

Figure 4 shows how a gear having an A.M. factor of 0.52 is deformed during rolling. The sign  $\nabla$  indicates a contact point on the tooth profile. The contact point on the tooth begins from the driven side at tooth tip and ends at the follower side at the tooth root. The load is 9.8 kN. At points A and B, the amount of deformation on the tooth profile contacted with the tool is positive. At point C, the gear rotates slightly from point B and a concave shape of the tooth appears at the pitch point on the tooth profile. Here, it is observed that the deformation of the driven side changes from positive to negative. The tooth profiles at points D and E show very little difference from the profile at point C.

Figure 5 shows the plastic deflection  $\delta_x$ . When the load is 9.8 kN, and the gear rotates from point A to point B, the plastic deflection is very small.

At point C, the plastic deflection grows large at the dedendum. The deflection of the dedendum at point C is unlike at point B and is inverted from positive to negative.

While the gear rotates from point B to point C, the heights of contact point on the driven side and the follower side are inverted near the pitch point. Here, the change in the direction of the dedendum corresponds to the tooth profile at point C in Figure 4. When the gear rotates from point C to point E in Figure 5, the tooth profiles at points D and E show very little difference from that at point C.

Figure 6 shows the radial elongation  $\delta_y$ . The tooth shows no elongation at point A. The tooth is slightly elongated at point B and is elongated more on the dedendum at point C. The elongation does not change when the mating progresses further.

Figure 7 shows the plastic strain  $\epsilon_y$  calculated from the results shown in Figure 6. The strain is nearly zero at points A and B and becomes very large at point C. The maximum strains are 0.2% and 0.9% when the loads are 9.8 kN and 14 kN, respectively. These results indicate that the plastic area reaches the center of the tooth near the pitch point where the heights of the contact point on the driven side and the follower sides are inverted. When the gear rotates from point D to point E, the strain at these points is nearly zero.

Figure 8 shows the deformation process in which the A.M. factor is zero. Results would likely be similar for values of A.M. factor up to about 0.4 based on the results of Uematsu (Ref. 7). In positions A and B, the tooth profile of the follower side contacts the tool, and the amount of deformation on the rolled part is in the positive direction. In position B, the tooth profile of the driven side has not yet come in contact with the tool. However,

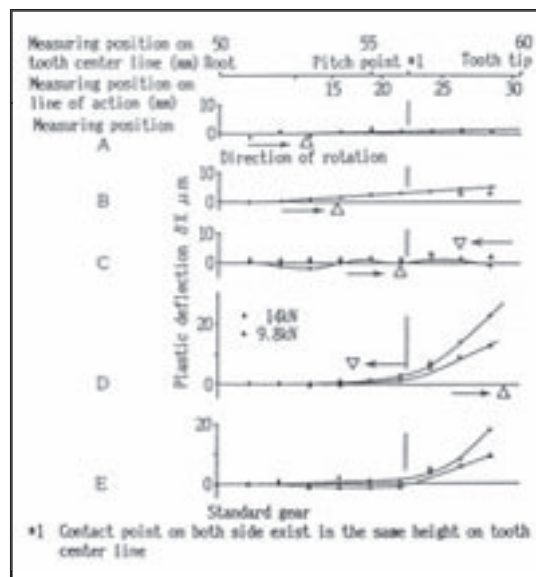


Figure 9—Plastic deflection of tooth.

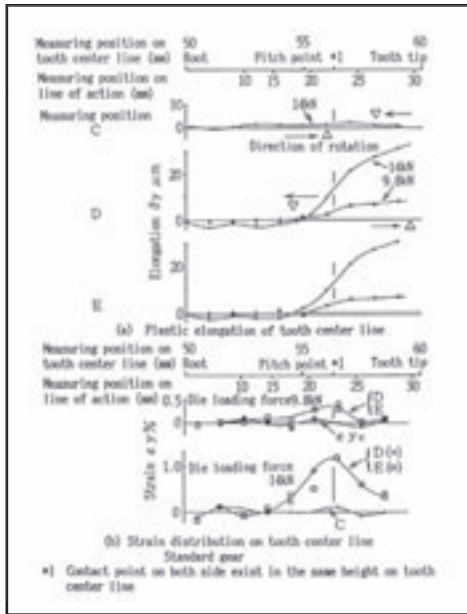


Figure 10—Plastic elongation on tooth center line.

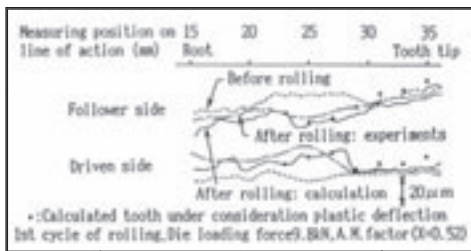


Figure 11—Calculated tooth's plastic deflection based on experimental results.

the tooth profile has been deformed in the negative direction before the tooth comes in contact with the rolling tool.

At position C, the tooth profile of the driven side begins to contact with the tool, and the negative deformation that appeared in position B is disappearing. The tooth profiles on both sides also contact with the tool, and the amounts of deformation on the driven side have a positive direction.

In position D, the amount of deformation on the driven side decreases and this tooth profile has been deformed more negatively than before rolling. In position E, the tooth contact has finished on both sides. The amount of deformation on the follower side that appeared in position D again decreases.

Figure 9 shows the plastic deflection of the tooth in rolling. The change of the plasticity deflection corresponds well to the tooth profile shown in Figure 8. When the tooth contact occurs on the tooth profile of one side as shown in positions A and B, the plastic deflection appears on the tooth root, and the elongation in the interval is small. When the tooth contact crosses near the pitch point as shown in positions C and D, the deflection in the addendum becomes bigger.

Figure 10 shows the elongation, and the plastic strain between points C and D are shown in Figure 9. When the tooth contact crosses near the pitch point as shown in positions C and

D, the elongation in the addendum becomes bigger. When the load is 9.8 kN, the strain becomes more than 0.2%. When it's 14 kN, the strain becomes 1.2%. As a result, the plastic region spreads near the pitch point on the central part of the tooth.

#### Formation Mechanism of Pressure Angle Error.

Plastic deflection and elongation in finish rolling were confirmed by the experimental result described above. Plastic deflection that appears in the addendum is affected by the transfer direction of the contact point on the tooth. The transfer direction of the contact point is decided by the direction of rotation. Therefore, as the tooth bends to the driven side, the amount of deformation on the tooth profile decreases on the driven side and increases on the follower side. The elongation appearing on the addendum decreases the amount of deformation on both tooth sides.

The amount of deformation on the tooth profile consists of the components:  $\delta P_d$ ,  $\delta P_f$ ,  $\delta_x \cos \theta$ ,  $\delta_y \sin \theta$  where  $\delta P_d$ ,  $\delta P_f$  is the amount of deformation,  $\delta_x \cos \theta$  is the plastic deflection,  $\delta_y \sin \theta$  is the plastic elongation, and  $\theta$  is the pressure angle. The total amount of deformation  $Y_d$  of the driven side and  $Y_f$  of the follower side will consist as following:

$$\begin{aligned} Y_d &= \delta P_d - \delta_x \cos \theta - \delta_y \sin \theta \\ Y_f &= \delta P_f + \delta_x \cos \theta - \delta_y \sin \theta \end{aligned} \quad (2)$$

Then, the result of the calculation based on Equation 2 is added to the tooth profile in which the deformation was calculated, and the pressure angle error is examined.

Figure 11 shows the result. The tooth profiles represented by the broken, dashed and solid lines are respectively the tooth profile before rolling, the experimental tooth and the calculated tooth.

The deformation correction value calculated by Equation 2 is shown by the black circles. The corrected tooth profile and the rolled tooth form agree to an accuracy of 1–2  $\mu\text{m}$ .

Therefore, the convex shape on the addendum of the driven side of the rolled tooth was not verified by the calculation with only the mean deformation being predicted by Equation 2. Similarly, the amount of deformation difference on the driven side and follower side is verified by the calculations using the same equation.

When the plastic region reaches the central part of the tooth, the pressure angle error is based on the second and third terms of Equation 2.

#### Tooth Profile Error at Low Load

In the above, the load was set to 9.8 kN, so that the deformation may easily appear in the tooth, and the mechanism in which the pressure angle error arose was examined. However, the conclusion obtained in this experiment may not always apply to the case in which the load is set at a lower value.

Figure 12 shows the results with a 5 kN load. The other experimental conditions are the pitch-line velocity of 8.5 m/min., and the number of total rolling cycles is 30. The

plastic deflection and plastic strain  $\epsilon_y$  on the center line is shown in Figure 12(a). This deflection is about 3  $\mu\text{m}$  near the pitch point and becomes about 12  $\mu\text{m}$  at the tooth tip. The strain remains at roughly 0.2% from the pitch point to the tooth tip. There is a maximum compressive strain of 0.2% on the dedendum, and the plastic region spreads to the central part of the tooth.

The profile of both sides of the rolled tooth is shown in Figure 12(b). The rolled tooth deformed almost uniformly along the hobbled tooth shape; the amount of plastic deformation ranges from 2–8  $\mu\text{m}$ . On the follower side, the concave shape at the pitch point has amplitude of about 30  $\mu\text{m}$ .

### Conclusion


In this paper, we have defined an evaluation method for tooth rolling and have established the formation mechanism of the pressure angle error. Analysis reveals two causes of the tooth profile error:

- 1.) When the tool approaches the work with a constant load, the number of mating teeth on the line of action varies, the normal load on the tooth changes with the number of mating teeth, and the concave type error occurs at the pitch point.
- 2.) When the tooth contact stress is very high near the pitch point, the plastic deformation extends inside the center of the tooth and the addendum deflects to the driven side.

Additional results of this study are as follows:

- 1.) The pressure angle error that appears in the addendum is the sum between plastic deflection on the addendum and the elongation in the same region and results in the concave shape at the pitch point.
- 2.) The deflection in the addendum decreases the deformation on the driven side and increases the deformation in the follower side (reverse effects).
- 3.) The elongation in the addendum decreases the amount of deformation in both teeth.
- 4.) This deflection and elongation arise when the contact point crosses near the pitch point on the right and left tooth profiles.
- 5.) The direction of deflection is decided according to the transfer direction of the contact point on the tooth surface, and the tooth deflects to the driven side regardless of the number of teeth and the addendum modification coefficient.

### Acknowledgments

This work was supported by grant No. RTI04-01-03 from the Regional Technology Innovation Program of Korea's Ministry of Commerce, Industry and Energy (MOCIE) and by the NURI Project at Gyeongsang National University. 

This paper was presented at the ASME/AGMA 2003 International Power Transmission and Gearing Conference, held Sept. 3–5, 2003, in Chicago, IL, and was published in *Proceedings of the 2003 ASME Design Engineering Technical Conferences & Computers and Information in Engineering Conference*. It's republished here with permission from ASME.

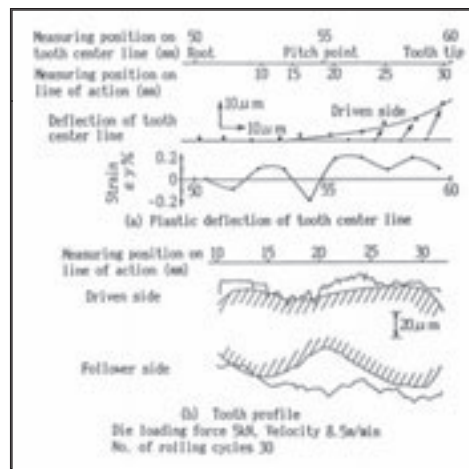


Figure 12—Tooth profile error and plastic deflection under low load rolling.

### References

1. DeVos, Leon N. "Roll Forming of Gears at Ford Motor Company," *Gear Design, Manufacturing and Inspection Manual*, AE-15, SAE International, 1990, pp. 335–343.
2. Terauchi, Y., M. Tahara and N. Wakaoka. "A Study of Rolling Finish," *Transactions of the Japan Society of Mechanical Engineers*, Vol. 43, 1977, pp. 4327–4336.
3. Tsutsumi, S., S. Tanaka and S. Senda. "Cold Rolling of Zigzag-Toothed Gears," *JSME International Journal, Series C*, Vol. 33, No. 2, 1990, pp. 251–255.
4. Ozaki, T., K. Funatsu and I. Fuchi. "Theoretical Analysis of Finish Rolled Gear Tooth Profiles," *Bulletin of JSME*, Vol. 29, No. 255, 1986, pp. 3182–3188.
5. Vasilchikov, V.M., et al. "The Effect of Gear Blank Throw on the Accuracy of Gear Rolling," *Russian Engineering Journal*, Vol. 57, No. 6, 1977, pp. 56–59.
6. Weck, M., W. Kong, J. Goebbelet and G. Bartsch, "Cold Rolling for Processing Involute Gears," International Symposium on Gearing & Power Transmissions, Tokyo, Japan, A-37, 1981, pp. 88–93.
7. Uematsu, S. "How to Occur Involute Profile Error in Finish Roll Forming of Spur Gears," *Transactions of Japan Society of Precision Engineering*, Vol. 54, No. 1, 1988, pp. 139–144.
8. Uematsu, S. and M. Kato. "Involute Profile Error in Finish Roll Forming of Spur Gears-Formation of Pressure Angle Error," *Transactions of the Japan Society of Precision Engineering*, Vol. 55, 1989, pp. 1839–1844.